Radiative Impact of Ozone on Temperature Predictability in a Coupled Chemistry–Dynamics Data Assimilation System

J. DE GRANDPRÉ AND R. MÉNARD

Atmospheric Science and Technology Directorate, Environment Canada, Dorval, Québec, Canada

Y. J. ROCHON

Atmospheric Science and Technology Directorate, Environment Canada, Toronto, Ontario, Canada

C. CHARETTE

Atmospheric Science and Technology Directorate, Environment Canada, Dorval, Québec, Canada

S. CHABRILLAT

Belgium Institute for Space Aeronomy, Brussels, Belgium

A. ROBICHAUD

Atmospheric Science and Technology Directorate, Environment Canada, Dorval, Québec, Canada

ABSTRACT

The objective of this study is to investigate the impact on temperature forecast of using ozone analyses for the computation of heating rates in a three-dimensional variational data assimilation (3D-Var) system with a coupled model. The system is based on a tropospheric–stratospheric forecast model that includes a comprehensive stratospheric chemistry module for online resolution of the dynamical, radiative, and photochemical interactions. The system assimilates conventional observations as well as temperature and ozone measurements from the Michelson Interferometer for Passive Atmospheric Sounding (MIPAS) instrument. Several data assimilation cycles have been performed over the period August–October 2003 to produce a set of analyses that have been used for launching an ensemble of 10-day forecasts. Temperature and ozone forecasts have been compared with MIPAS and radiosonde observations in different regions. Results show that, in the absence of ozone assimilation, the impact of using a prognostic ozone distribution for the computation of heating rates as opposed to monthly mean climatologies is generally neutral. With the addition of ozone assimilation, the improvement against a noninteractive assimilation system is systematic and occurs over a wide range of time scales throughout the lower stratosphere. The improvement on 6-h temperature forecasts is mainly seen in the Southern Hemisphere, where ozone analyses are in good agreement with observations. For 10-day forecasts, the impact of using ozone analyses is more important in the Northern Hemisphere, where it improves the temperature predictability by more than 1 day at 50 hPa. Comparisons with analyses also show a systematic reduction of the temperature root-mean-square errors and biases throughout the assimilation period. The overall results demonstrate that a comprehensive coupled 3D-Var system that incorporates the radiative feedback from ozone analyses can be used for improving temperature predictability throughout the stratosphere. Comprehensive approaches can be used as a benchmark for the development of linearized methods for improving temperature and ozone forecasting in the region.

Corresponding author address: Jean de Grandpré, Atmospheric Science and Technology Directorate, Environment Canada, 2121 Trans-Canada Highway, Dorval, QC H9P 1J3, Canada.
E-mail: jean.degrandpre@ec.gc.ca

1. Introduction

The development of stratospheric–tropospheric versions of numerical weather prediction (NWP) models provides the opportunity to produce global analyses of ozone on an operational basis (Jackson 2004; Morcrette 2003). Ozone analyses have been used to improve the assimilation of satellite radiances (Dethof 2003), for wind retrieval (Riishøjgaard 1996), for the computation of the UV forecast index (Long et al. 1996), for diagnosing dynamical processes in the lower stratosphere (Geer et al. 2006), and in climate studies to understand long-term trends in ozone and temperature (WMO 2007). The use of ozone analyses for the computation of heating rates can also improve temperature forecasts in the upper troposphere and lower stratosphere regions (Cariolle and Morcrette 2006).

Ozone–temperature interactions are determined by complex dynamical radiative and photochemical interactions, which vary in different regions. The impact of temperature on gas-phase ozone photochemistry is determined by the temperature sensitivity of numerous coupled photochemical reactions. The negative correlation between temperature and ozone in the upper stratosphere is mainly associated with the negative temperature dependency of the $O + O_2 + M \rightarrow O_3 + M$ reaction, which controls odd-oxygen partitioning and largely determines the ozone loss in the region (Jonsson et al. 2004). The radiative impact of ozone on temperature occurs through radiative transfer in the UV-to-visible and infrared parts of the solar spectrum (Cariolle and Morcrette 2006). Changes in ozone and temperature distributions perturb the radiative equilibrium, which induces changes in the residual circulation on a time scale of several months. Finally, ozone is advected and thus directly influenced by the wind field, especially in the lower stratosphere where its photochemical lifetime exceeds several months (Brasseur and Solomon 1986).

The complexity of the dynamical–radiative and photochemical interactions can be resolved with state-of-the-art coupled chemistry–climate models (CCMs) via the coupling between the different modules. CCMs are used in investigating the causes of changes of ozone and temperature in the recent past (Eyring et al. 2005) and for performing climate prediction on ozone recovery (Austin et al. 2003). CCM studies (de Grandpré et al. 2000; Sassi et al. 2005) show that the radiative impact of using a prognostic ozone distribution is significant and depends on the magnitude of the ozone photochemical lifetime, which increases from a few hours at the stratopause to several months at the tropopause. It is particularly significant in the lower stratosphere where the

ozone radiative forcing has a significant impact on temperature over the time scale of the forecast. CCM studies demonstrate the models' capability of representing ozone–temperature interactions throughout the middle atmosphere, which is an important issue for a wide range of applications.

For the purpose of NWP, the impact of ozone radiative feedback on temperature predictability within a 10-day time scale needs to be characterized. It mainly depends on the magnitude of the photochemical lifetimes and the radiative time scales that determine the relationship between ozone and temperature in different regions (Ward et al. 2000). Jackson (2004) and Morcrette (2003) have investigated the impact of ozone heating on temperature forecasts within data assimilation systems using linearized approaches for the representation of the photochemical ozone (e.g., Cariolle and Déqué 1986; McLinden et al. 2000). Both studies indicate that the use of ozone analyses for the computation of heating rates is generally positive, particularly in the lower stratosphere where the radiative relaxation time generally exceeds several weeks. Morcrette (2003) also reveals a deterioration of the results in specific regions, such as in the lower stratosphere of the Northern Hemisphere (NH) where a significant increase of temperature root-mean-square (RMS) errors is obtained. Such effects can be associated with several factors including the quality of ozone observations (e.g., Mathison et al. 2007), which has a large impact on the temperature predictability in various regions. The use of simplified chemistry on ozone interactive forecasts is another aspect of predictability issues that needs to be evaluated. To address it, the implementation of comprehensive approaches for resolving dynamical, radiative, and photochemical interactions can serve as a benchmark for evaluating more efficient methods used on an operational basis (Geer et al. 2006).

In this study, a comprehensive 3D-Var tropospheric–stratospheric assimilation system with a coupled chemistry–dynamical model has been used to evaluate the radiative impact of ozone modeling and assimilation on temperature predictability. This coupled assimilation system (Ménard et al. 2007) has been developed in the framework of a sponsored project by the European Space Agency (ESA) under the partnership of Environment Canada (EC), the Belgian Institute for Space Aeronomy (BIRA-IASB), the German Institute for Meteorology and Climatology (IMK) and York University (Canada). The assimilation system is based on a fully coupled model with a lid at 0.1 hPa and in which ozone photochemistry is computed online at every dynamical time step and used for the computation of ra-

diative processes. The assimilation system uses the temperature and ozone limb sounding measurements from the Michelson Interferometer for Passive Atmospheric Sounding (MIPAS) and the standard operational data.

The study presents the results of different assimilation cycles over the period August–October 2003 to evaluate the overall benefits of using a fully comprehensive coupled assimilation system on temperature predictability. The results are compared against MIPAS and radiosonde measurements in the extratropical regions where temperature responses are significant. Section 2 gives an overview of the assimilation system, and sections 3 and 4 present respectively the results of temperature predictability over short- and medium-range time scales. Conclusions are presented in section 5.

2. The assimilation system and experiments

The coupled assimilation system presented in this study—the Canadian Global Environmental Multiscale (GEM) model in combination with the Belgium Atmospheric Chemistry module (BACH), hereinafter GEM-BACH)—is based on the stratospheric version (GEM-Strato) of the Canadian GEM model (Côté et al. 1998). The Hines scheme (1997a,b) is used for the parameterization of momentum deposition by subgrid-scale nonorographic gravity waves; the model also includes a Rayleigh-drag sponge layer that ramps up smoothly above the stratopause to prevent downward reflection at the upper boundary. The model has been coupled online with a comprehensive module of stratospheric chemistry developed at BIRA-IASB. The model has 80 levels, including 27 in the stratosphere, and runs at a horizontal resolution of 1.5° with a lid at 0.1 hPa. It uses semi-implicit and semi-Lagrangian numerical techniques optimized to handle a large number of advection equations for the transport of species. Radiative processes are computed according to the correlated-k distribution approach (Li and Barker 2005), which has the accuracy of a line-by-line code. It uses as input either an interactive ozone distribution or monthly mean climatologies from Fortuin and Kelder (1998), which are merged with *Upper Atmosphere Research Satellite* (*UARS*) measurements (available at atmos.sparc.sunysb.edu) above 0.5 hPa (hereinafter FK-UARS).

The Belgium Atmospheric Chemistry module is the foundation of the Belgium Assimilation System of Chemical Observations from the *Environmental Satellite* (*Envisat*) chemical transport model (BASCOE CTM; Daerden et al. 2007) and assimilation system (Geer et al. 2006; Errera et al. 2008). It includes 57 species that interact through 143 gas-phase, 48 photoly-

sis, and 9 heterogeneous reactions. The chemistry solver is built by the Kinetic PreProcessor (Damian et al. 2002) and is integrated using a third-order Rosenbrock solver (Hairer and Wanner 1996). The chemical and photodissociation rates follow the Jet Propulsion Laboratory compilation by Sander et al. (2003).

The 3D-Var (Gauthier et al. 1999a, b) FGAT (First Guess at Appropriate Time) assimilation system is used in this study. In all experiments, conventional meteorological observations [radiosondes, surface observations, aircraft winds, and radiances from Advanced Microwave Sounding Units (AMSUs)] are assimilated. This assimilation system has been extended to include the assimilation of chemical constituents from MIPAS and also incorporates a bias correction of AMSU-A stratospheric channels using MIPAS temperatures as a reference. The ozone background error statistics are set for univariate assimilation; the characterization of error variances has been done following the approach of Hollingsworth and Lönnberg (1986), whereas the NMC method (Parrish and Derber 1992) is used for temperature.

The MIPAS instrument aboard the *Envisat* mission placed in orbit on 1 March 2002 (Raspollini et al. 2006) is a Fourier transform spectrometer performing slow downward scans and measures the complete spectrum of limb emission from 4.15 to 14.6 microns (Fischer and Oelhaf 1996). It offers a global geographical and temporal coverage and provides day and night measurements with a 3-km vertical resolution. A spectrum is acquired every 4.6 s for each of the 17 tangent altitudes, giving about 1000 profiles per day starting at an altitude of 68 km down to 6 km. The field of view is 3 km × 30 km with a resolution of 500 km along track and about 2800 km across track at the equator. The bias of the MIPAS temperature profiles is generally smaller than 2 K (Ridolfi et al. 2007) and typical biases and RMS errors for ozone are in the range of 5%–15% (Geer et al. 2006; Baier et al. 2005).

Table 1 describes the different assimilation cycles used for assessing specific aspects of the temperature–ozone interactions throughout the lower stratosphere. Experiments A1 and A2 were conducted to evaluate the radiative impact of incorporating a prognostic ozone distribution in the model, whereas experiments B1 and B2 were used to determine the impact of including ozone assimilation. Experiments C1 and C2 were performed to evaluate the benefit of ozone assimilation on temperature analyses and predictability in an operational context in which conventional observations and MIPAS measurements are assimilated. The different assimilation cycles do not cover the same time pe-

TABLE 1. List of configurations of the different assimilation experiments.

Expt identifier	Description of 3D-Var FGAT experiments
A1	Experimental name: AT420300
	Assimilation of conventional observations and MIPAS temperature without Television and Infrared Observation Satellite Operational Vertical Sounder (TOVS) AMSU-A stratospheric channels (channels 9–14).
	Use of FK-UARS ozone climatology in the radiation.
	Assimilation period: 11 Aug–5 Sep 2003
A2	Experimental name: AT420304
	Same as A1 including the ozone radiative feedback from prognostic ozone.
B1	Experimental name: K3BCS304
	Assimilation of conventional observations including TOVS AMSU-A stratospheric channels (channels 9–14) and without MIPAS temperature.
	Use of FK-UARS ozone climatology in the radiation.
	Assimilation period: 11 Aug–5 Sep 2003
B2	Experimental name: K3BCS310
	Same as B1 including the radiative feedback from prognostic ozone and the assimilation of MIPAS ozone measurements.
	Radiative feedback from ozone analyses.
C1	Experimental name: VT410321
	Assimilation of conventional observations including MIPAS temperature
	Use of FK-UARS ozone climatology in the radiation.
	Assimilation period: 11 Aug–5 Oct 2003
C2	Experimental name: VT410322
	Same as C1 including the radiative feedback from prognostic ozone and the assimilation of MIPAS ozone measurements.

riod, but the results have been averaged over 11 August to 5 September 2003 both to facilitate comparisons between the different experiments and to avoid the period 6–20 September, during which MIPAS observations were not available.

3. Short-term temperature and ozone forecast

The impact of the ozone radiative feedback on short-term (6 h) temperature and ozone forecasts with and without assimilation has been investigated by comparing different assimilation cycles in which temperatures have been assimilated. These comparisons allow us to separately evaluate the impact of using a prognostic ozone distribution instead of monthly mean climatologies and the impact of assimilating ozone (or not) on temperature predictability.

Figure 1 shows the comparison between experiment A1, which uses the FK-UARS ozone climatology in the computation of heating rates, and experiment A2, which uses instead the GEM-BACH prognostic ozone distribution without assimilation. The panels present mean O − F temperature and ozone differences and standard deviations, where O indicates observations taken from MIPAS and F denotes 6-h forecasts from the assimilation experiments. Symbols on the right indicate that differences between both experiments are

significant at the 95% level or higher according to the t test for the mean and the f test for the variance. For experiment A1, ozone forecasts (F) refer to the FK-UARS climatology, which is used in the computation of heating rates.

The results show that the FK-UARS ozone climatology is generally in good agreement with observations throughout the stratosphere, with global mean differences within 4% of the MIPAS values. Above 10 hPa, results reveal the increase of an ozone deficit for the prognostic ozone that increases with height and reaches 15% at the stratopause. This model bias is attributed to a misrepresentation of the photochemical ozone loss, which can result from several factors including the transport of ozone precursors such as nitrous oxide and CFCs, the photodissociation of constituents, and the representation of the chemical processes (Eyring et al. 2005). The significant reduction of the standard deviations nevertheless indicates the positive impact of using a prognostic ozone distribution in regions controlled by photochemistry. Below 10 hPa, the overall improvement of the mean differences and standard deviation is associated with the representation of transport processes, which mainly determine the ozone distribution in the region. The assimilation of meteorological fields is sufficient in this case to maintain a realistic representation of ozone over a period of several weeks in the absence of ozone assimilation.
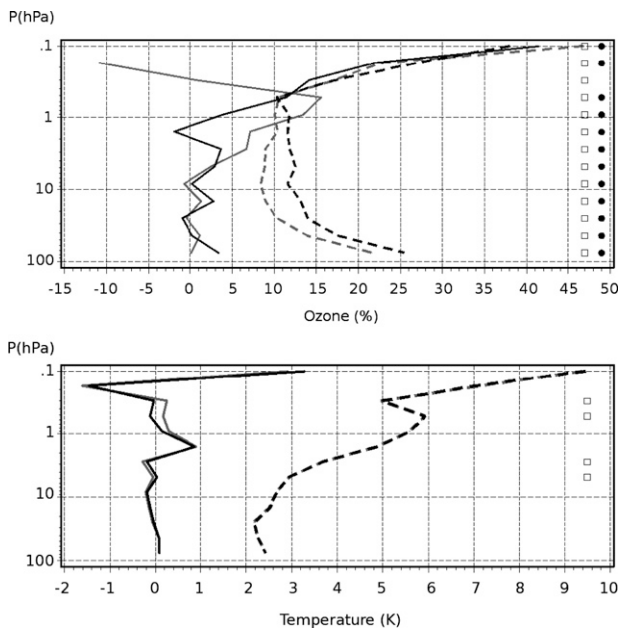
FIG. 1. Observation minus 6-h forecast (O − F) global mean differences (solid) and standard deviation (dashed) for (top) ozone and (bottom) temperature; results from the A1 experiment using the FK-UARS ozone climatology (black) and from the A2 experiment using the prognostic ozone (gray) for the period 11 Aug–5 Sep 2003. The ozone profile for A1 represents the FK-UARS climatology instead of a forecast. The squares and circles appearing on the right indicate that differences are significant at the level of 95% or more using the t test for the mean and the f test for the standard deviation.

The bottom panel presents the impact of incorporating the ozone radiative feedback on 6-h temperature forecasts in the absence of ozone assimilation. It shows differences with statistical significance under the 95% level in most regions except for a slight warming around 3 hPa and cooling around 0.3 hPa. These results reveal that using an ozone interactive model has little impact on short-term temperature forecasts; instead, the impact is more significant in the context of CCM studies. Differences in the radiative forcing associated with ozone change for the A1 and A2 experiments appear largely overwhelmed by the effect of assimilating temperatures.

The impact of the ozone radiative feedback on temperatures within the assimilation system is more significant when ozone measurements are assimilated. This can be demonstrated by comparing the results of an assimilation cycle that uses monthly mean ozone climatologies (B1) with a cycle that uses a prognostic ozone distribution with the assimilation of MIPAS measurements (B2). The O − F comparison in Fig. 2 shows the response of both assimilation cycles in the various re-

gions for both temperature and ozone. As previously indicated, ozone forecasts (F) for B1 refer to the FK-UARS climatology, which is used in the computation of heating rates. For ozone, the results are presented in mixing ratio units to facilitate evaluation in the lower stratospheric and upper tropospheric regions.

Results show significant differences between the NH summertime and the Southern Hemisphere (SH) wintertime regimes that are mainly associated with the seasonal variations in the ozone photochemical lifetime. In the SH, ozone 6-h forecasts are significantly lower than climatological values and appear to be in very good agreement with MIPAS throughout the stratospheric domain. In the NH, the agreement with MIPAS is slightly worse than in the SH, and biases in the ozone forecasts start developing around 5 hPa as photochemistry becomes more important. The comparison indicates a good agreement between ozone forecasts and MIPAS in most regions throughout the stratospheric domain, which shows the overall capability of the system to assimilate ozone in different photochemical and dynamical regimes. The largest differences between ozone forecasts and MIPAS observations are obtained in the stratopause region where the ozone photochemical lifetime is smaller than the 6-h model integration period. Under this condition, ozone values are close to those obtained without ozone assimilation (see Fig. 1).

The left panels present the impact of the associated ozone radiative forcing on the temperature in the different regions. The temperature forecasts are compared against MIPAS measurements, which are not assimilated and can be used as independent dataset to some degree, noting that a bias correction of stratospheric AMSU-A channels based on MIPAS temperature has been applied. In the SH, ozone assimilation generally results in an improvement of temperature forecasts down to 20 hPa (even though the improvement is small below 2 hPa), thus demonstrating the capability of the coupled assimilation system to resolve the photochemical–radiative coupling between temperature and ozone over an extended domain.

The impact of ozone assimilation on temperature in different regions depends on the relative importance of the ozone photochemical lifetime and the radiative time scale. The improvement obtained in the SH is attributed to the wintertime increases of the ozone photochemical lifetime throughout the stratosphere, which contributes to the enhancement of the associated radiative forcing over the forecast time scale. Results show that in the NH summertime where the photochemical and radiative interactions are stronger, ozone assimilation can contribute to the deterioration of the tempera-
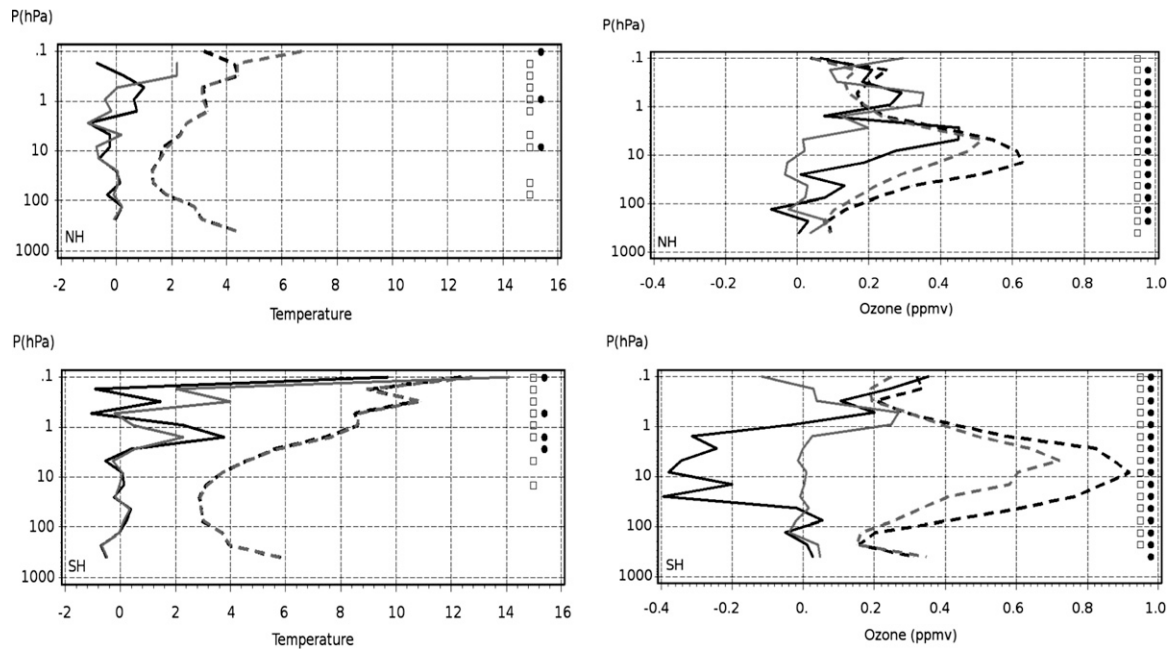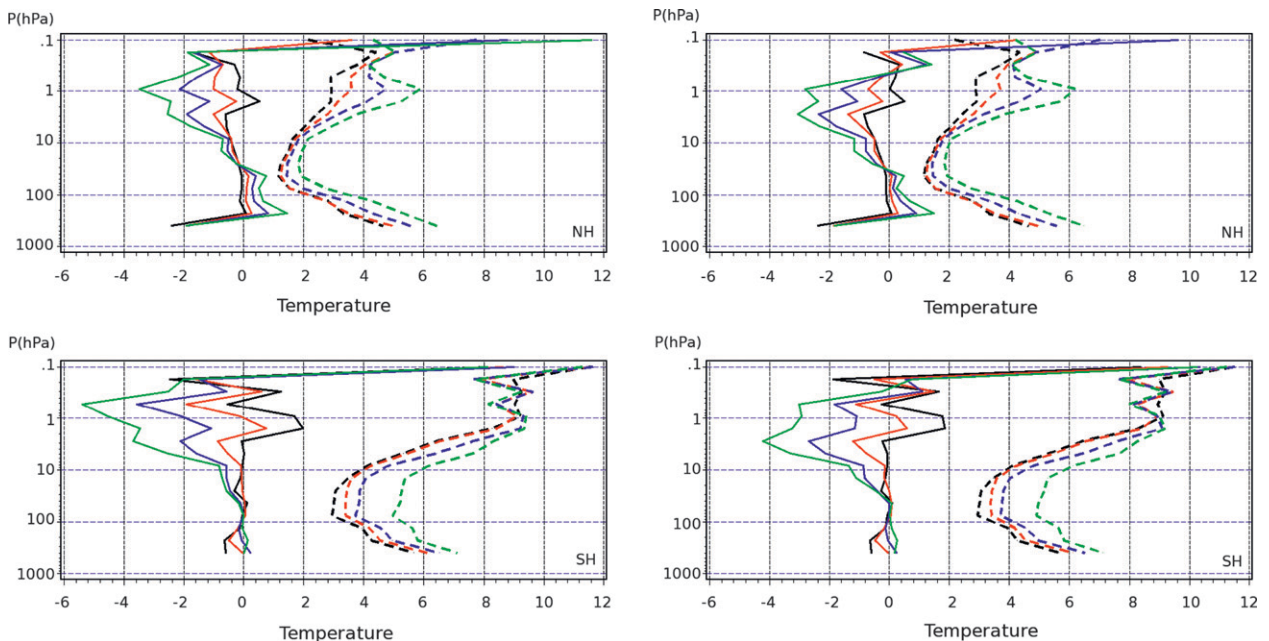
FIG. 2. Observation minus 6-h forecast (O − F) mean differences (solid) and standard deviation (dashed) for (left) temperature and (right) ozone; results from the B1 experiment using the FK-UARS ozone climatology (black) and from the B2 experiment using the prognostic ozone (gray). (top) NH (20°–90°N) and (bottom) SH (20°–90°S) for the period 11 Aug–5 Sep 2003. The ozone profile for B1 represents the FK-UARS climatology instead of a forecast. The squares and circles appearing on the right indicate that differences are significant at the level of 95% or more using the *t* test for the mean and the *f* test for the standard deviation.

FIG. 3. Observation minus 24-, 48-, 120-, and 240-h forecasts (O − F) mean temperature differences (solid) and standard deviation (dashed). Results from (left) noninteractive forecast using C1 analyses and (right) interactive forecast using C2 analyses (right) for 24- (black), 48- (red), 120- (blue), and 240-h (green) temperature forecasts; (top) NH (20°–90°N) and (bottom) SH (20°–90°S) for 11 Aug–5 Sep 2003.

ture analyses that is observed at 10 hPa. Univariate assimilation for temperature and ozone may not be sufficient in such a regime for preventing spurious photochemical and radiative adjustment within the coupled model.

Results finally demonstrate that ozone assimilation produces a significant temperature increase in the stratopause region between 3 and 0.5 hPa in both hemispheres, in better agreement with MIPAS observations in that region. Above 0.5 hPa, temperature forecasts are generally colder for the interactive cycle, which contributes to the production of more ozone than would otherwise be prescribed from the climatological values.

4. Temperature and ozone predictability

The impact of incorporating the ozone radiative feedback on temperature forecasts from 1 to 10 days has been evaluated by comparing an ensemble of noninteractive and interactive forecasts. Noninteractive forecasts were launched from a set of analyses obtained from an assimilation cycle (C1) that is based on a noninteractive model and includes the assimilation of MIPAS temperatures. For interactive forecasts, analyses come from an assimilation cycle (C2) that is based on a coupled model and includes the assimilation of temperature and ozone from MIPAS. Both sets of analyses include the assimilation of conventional observations. Forecasts were launched every 12 h and compared against MIPAS measurements, radiosondes, and analyses over the period 11 August to 5 September 2003 during which MIPAS data are available.

a. Comparison with MIPAS

Figure 3 compares the 24-, 48-, 120-, and 240-h temperature forecasts with MIPAS observations in the NH and SH regions for both assimilation cycles. Results present the growth of forecast error with time, which varies significantly over the different regions. Panels show a widespread warming throughout the stratosphere with temperature biases after 10 days reaching only 1 K at 10 hPa but becoming as large as about 4–5 K in the SH stratopause region. This warming is driven by solar heating and infrared cooling, which pull the model away from the dynamical–radiative equilibrium determined by the analyses. Results indicate that the standard deviation of the temperature forecast with respect to MIPAS observations in the SH is significantly larger than in the NH between 10 and 100 hPa. This is associated with the larger planetary wave activity observed in wintertime producing a rapid increase of the stan-
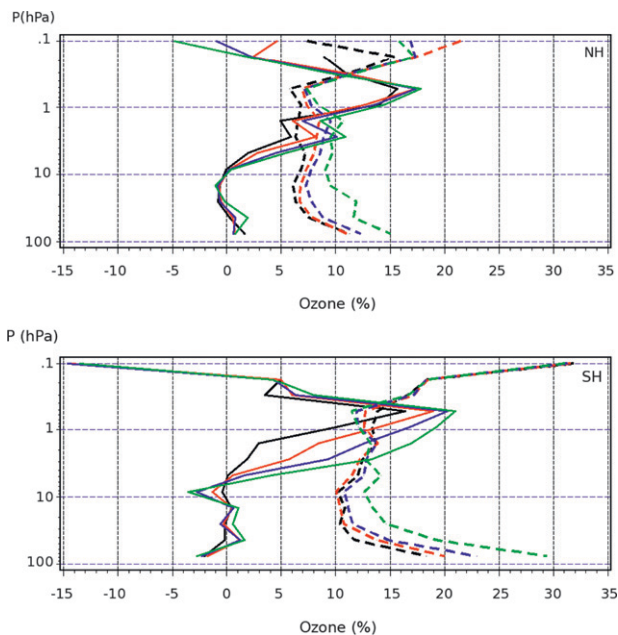

FIG. 4. Observation minus forecast (O − F) mean ozone differences (solid) and standard deviation (dashed). Results from interactive forecasts using C2 analyses for 24- (black), 48- (red), 120- (blue) and 240-h (green) ozone forecasts; (left) NH (20°–90°N) and (right) SH (20°–90°S) for 11 Aug–5 Sep 2003.

dard deviation with time, which is particularly strong in the SH lower stratosphere region. In the stratopause region, the radiative feedback associated with the modeled ozone deficit is more significant and has an impact on interactive forecasts: they appear colder than noninteractive forecasts and closer to MIPAS observations. In the lower stratosphere between 100 and 30 hPa, ozone interactive forecasts provide slightly better agreement with MIPAS temperatures, likely because of a better representation of ozone and associated heating (Fig. 2).

Figure 4 compares the 24-, 48-, 120-, and 240-h ozone forecasts launched from C2 analyses with MIPAS observations in both hemispheres. The most significant effect is the growth of ozone bias in the upper stratosphere associated with the presence of an ozone deficit in the model, which develops rapidly with time and reaches 10% at 3 hPa. This bias is not entirely due to the model representation of the photochemical processes because the warm temperature bias in the region also contributes to the enhancement of the ozone chemical loss. The ozone deficit in the upper stratosphere has an impact just above 10 hPa in the SH where it produces an ozone increase of ~4%, which is associated with a self-healing effect. It contributes to the warming of the region, which is mainly responsible for the temperature bias obtained at 10 hPa for the inter-
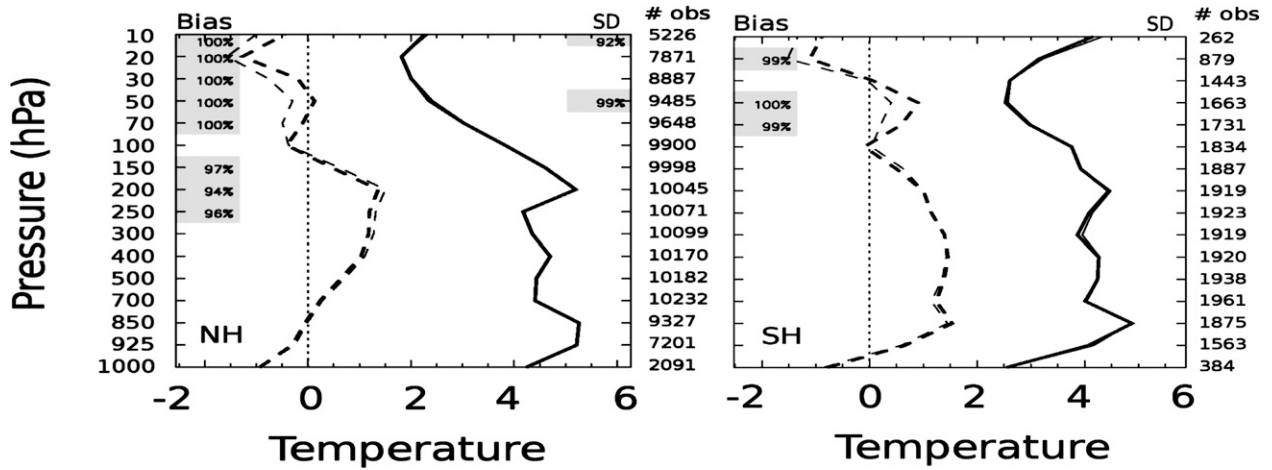
FIG. 5. Radiosonde observations minus 10-day forecast (O − F) mean temperature differences (dashed) and standard deviation (solid). Results from noninteractive forecasts using C1 analyses (black) and from interactive forecasts using C2 analyses (gray); (left) NH (20°–90°N) and (right) SH (20°–90°S) for 11 Aug–5 Sep 2003. The number of observations per level is indicated on the right axis. On the left and right axes are indicated respectively the level of significance for the differences of the mean and standard deviation at the level of 90% or more.
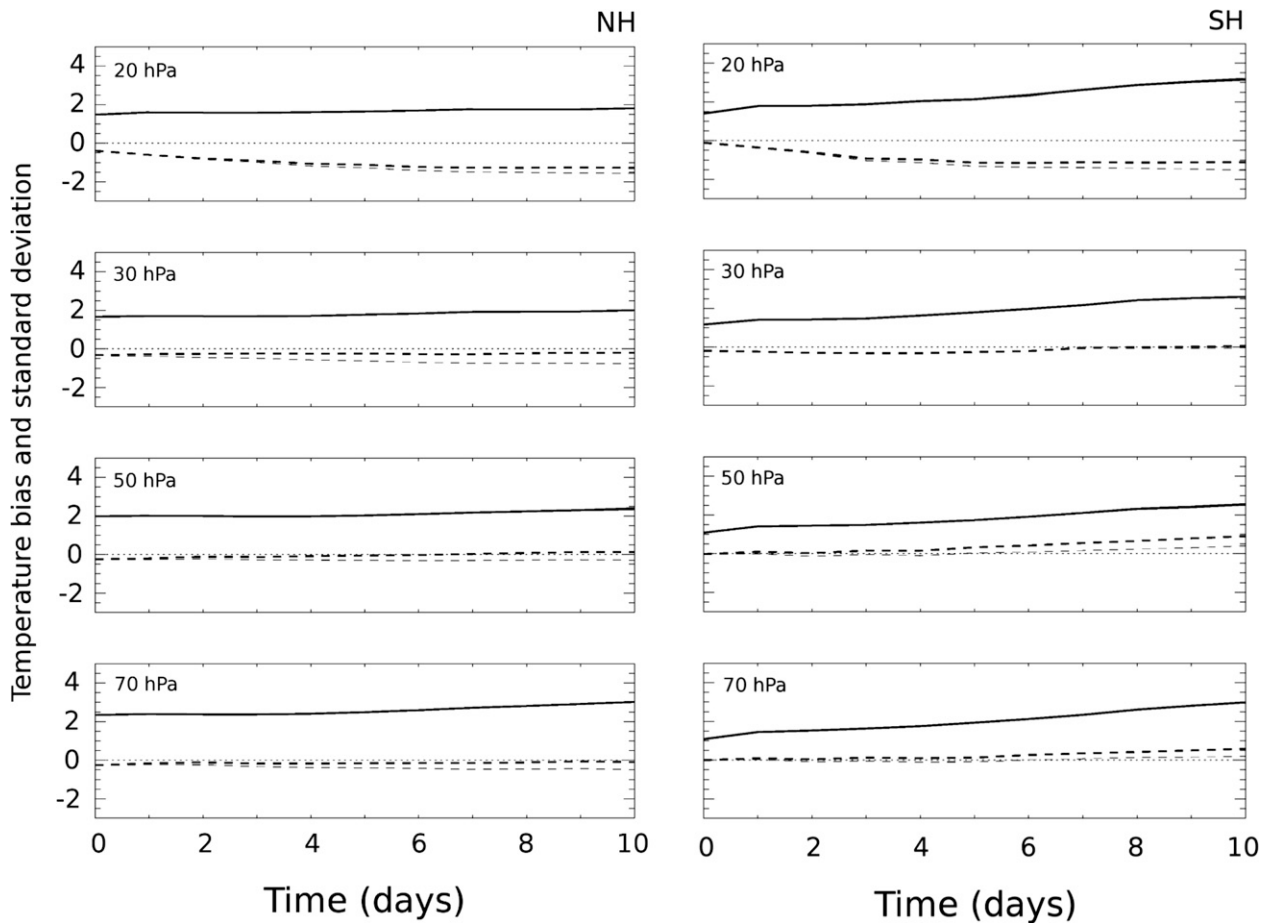

FIG. 6. Time series of radiosonde observations minus forecast (O − F) mean temperature differences (dashed) and standard deviation (solid) for (top to bottom) 20–70 hPa. Results from noninteractive forecasts using C1 analyses (black) and interactive forecasts using C2 analyses (gray); (left) NH (20°–90°N) and (right) SH (20°–90°S) for 11 Aug–5 Sep 2003.
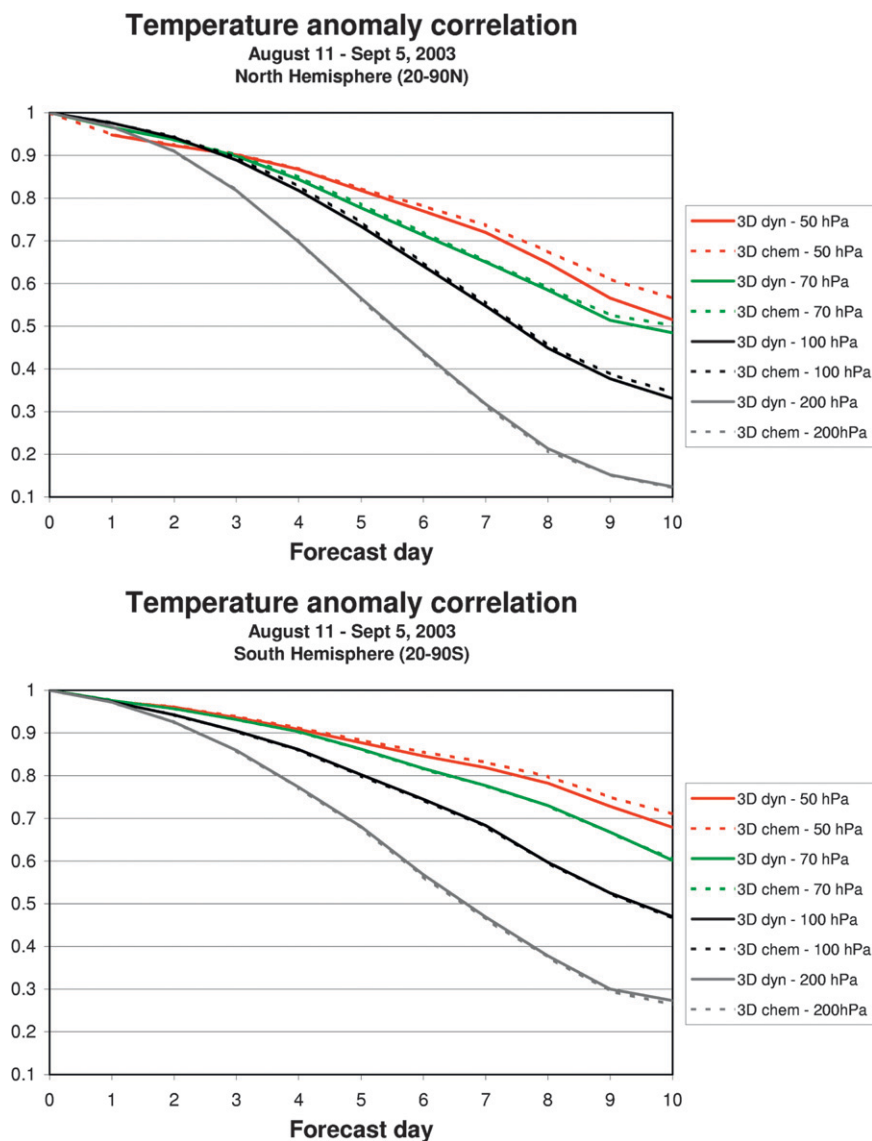
FIG. 7. Temperature anomaly correlation at 50 (red), 70 (green), 100 (black), and 200 hPa (gray) for noninteractive forecasts using C1 analyses (solid) and interactive forecasts using C2 analyses (dashed); (top) NH (20°–90°N) and (bottom) SH (20°–90°S) for 11 Aug–5 Sep 2003.

active forecasts. In the NH the ozone deficit in the upper stratosphere is much smaller, and there is no sign of any self-healing effect in the ozone profile.

In the NH below 10 hPa, the interactive assimilation system (C2) gives temperature and ozone biases that have the same sign as expected from theory (i.e., negative between 10 and 30 hPa and positive below). These results reveal consistencies in MIPAS measurements and the potential of using independent temperature and ozone measurements for detecting model biases. These results also indicate the model capability to represent the radiative and photochemical interactions that determine the correlation between both quantities

in the region. In the SH, the warm bias above 30 hPa is not associated with any significant ozone bias because of the weaker impact of the wintertime radiative feedback. In the upper stratosphere, the ozone photochemical lifetime is much smaller than radiative time scales and temperatures generally determine the ozone distribution. Temperature forecasts in both hemispheres are generally warmer than MIPAS even though ozone analyses in the SH are significantly smaller than climatological values (Fig. 2). Warm biases in temperature forecasts throughout the region contribute to the deterioration of ozone forecasts, particularly in the SH where temperature biases are larger.

b. Comparison against radiosondes

Figure 5 compares both ensembles of 10-day temperature forecasts against radiosonde observations in both hemispheres. The results show minor differences for the standard deviations but significant differences for temperature biases. The similarity between the experiments for the standard deviations can be due to several factors. It may suggest that the observation error is much larger than the model error or that the correlation between model and observation errors is similar for both experiments (Murphy and Epstein 1989). Bias differences will serve in this case to determine the relative performance of both assimilation cycles.

Results show that ozone interactive forecasts are warmer than noninteractive forecasts throughout the lower stratosphere, with temperature differences reaching 0.5° at 50 hPa. In the Southern Hemisphere below 30 hPa, the agreement against radiosondes improves with the use of an interactive system, whereas at higher levels a better agreement is obtained with the noninteractive system. In the NH, the interactive system generates a warm bias throughout the entire lower stratosphere region. The temperature signal is also significant in the extratropical lowermost stratosphere (between 100 and 250 hPa) where ozone interactive forecasts produce a slight increase of temperature biases.

The time evolution of temperature biases and standard deviations at various heights throughout the forecast period are shown in Fig. 6. Results show that above 30 hPa, biases are developing in both assimilation cycles with a stronger magnitude for interactive forecasts. The magnitude of the photochemical ozone loss, which exceeds a few percent per day in the region, can contribute to pull the temperature forecast away from the (assimilated) observations for the C2 interactive cycle. At 30 hPa and below, drifts of the forecast means are smaller but the differences between both forecast ensembles remain significant. In the SH, the temperature drift below 50 hPa is more pronounced for the C1 noninteractive cycle, which largely explains the larger discrepancies against radiosondes obtained in the region. In the NH, the presence of a drift in the mean temperatures similarly explains the better agreement with radiosondes obtained for the noninteractive forecasts. Both effects can be associated with the period of adjustment that is necessary for reaching dynamical–radiative equilibrium within the model using climatological ozone values.

The reduction of the mean temperature biases in the forecast for the coupled assimilation system is associated with a better representation of the radiative and photochemical interactions in the production of temperature and ozone analyses. In this case, ozone analyses determine the quality of temperature forecasts given the long photochemical lifetime of ozone in the lower stratosphere region. Positive biases in the MIPAS ozone analyses (Geer et al. 2006) can contribute to the generation of a warm bias in the ozone interactive forecast that is seen in Fig. 5. These results show the necessity of assimilating other sources of ozone measurements for investigating the benefit of ozone assimilation for temperature predictability.

c. Comparison against 3D-Var analyses

The two ensembles of forecasts have been compared with analyses using standard diagnostics of the mean error, RMS error, and anomaly correlation using the following definitions (WMO 1998):

$$\text{Mean error} \quad M_{f,v} = \frac{\sum_{i=1}^{n} (x_f - x_v)_i \cos\varphi_i}{\sum_{i=1}^{n} \cos\varphi_i}, \tag{1}$$

$$\text{RMS error} \quad \text{rmse} = \sqrt{\frac{\sum_{i=1}^{n} (x_f - x_v)_i^2 \cos\varphi_i}{\sum_{i=1}^{n} \cos\varphi_i}}, \quad \text{and} \tag{2}$$

$$\text{Anomaly correlation} \quad r = \frac{\sum_{i=1}^{n} (x_f - x_c - M_{f,c})_i (x_v - x_c - M_{v,c})_i \cos\varphi_i}{\sqrt{\sum_{i=1}^{n} (x_f - x_c - M_{f,c})_i^2 \cos\varphi_i} \sqrt{\sum_{i=1}^{n} (x_v - x_c - M_{v,c})_i^2 \cos\varphi_i}}, \tag{3}$$

Temperature anomaly correlation
August 11 - Sept 5, 2003
North Hemisphere (20-90N)

Temperature anomaly correlation
August 11 - Sept 5, 2003
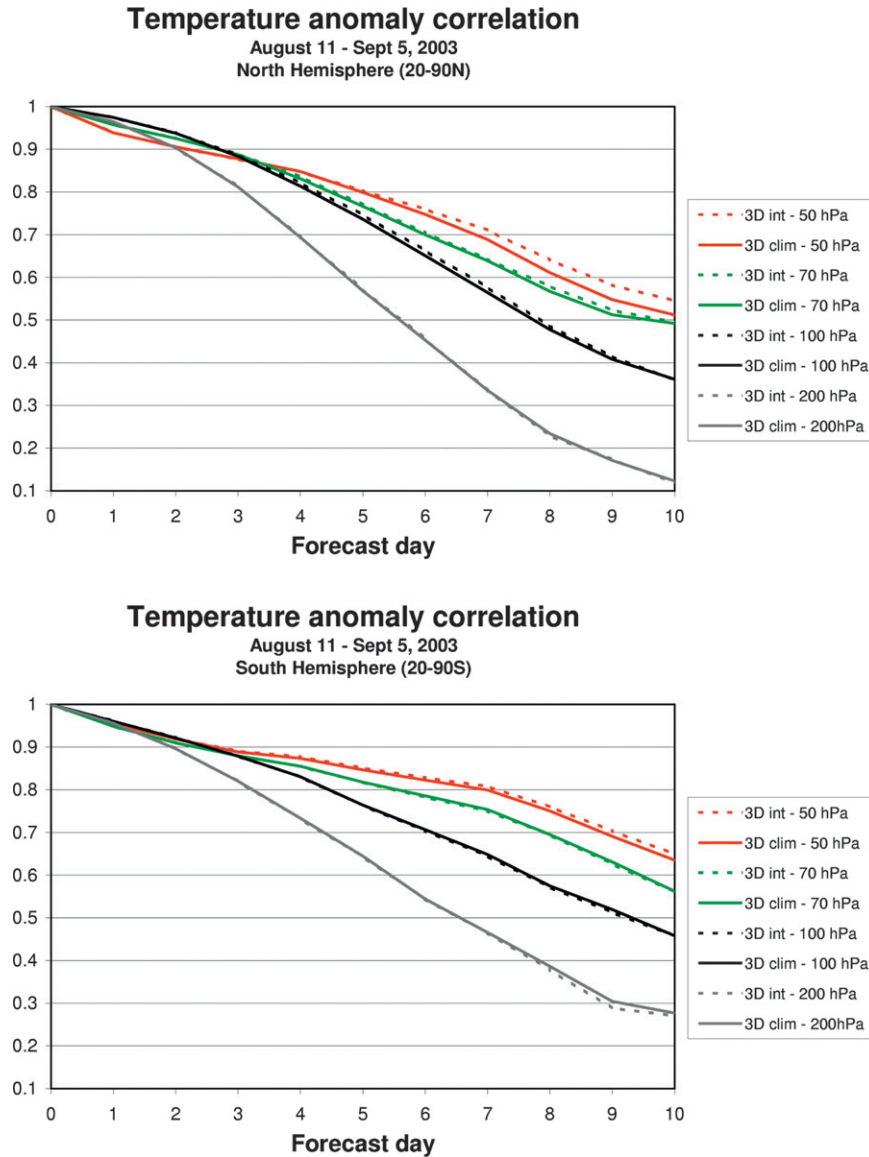### South Hemisphere (20-90S)

FIG. 8. As in Fig. 7, but for A1 and A2 analyses.

where

x_f is the forecast value of the parameter,

x_v is the corresponding verifying value (observed),

n is the number of grid points in the verification area,

φ is the latitude of the grid point i,

x_c is the climatological value of the parameter,

$M_{f,c}$ is the mean value over the verification area of the forecast climate anomalies, and

$M_{v,c}$ is the mean value over the verification area of the analyzed climate anomalies.

Figure 7 evaluates temperature forecasts in terms of anomaly correlation at 24-h intervals in both hemi-

spheres and at different altitudes. Results show that the model predictability throughout the stratosphere is large and varies significantly with altitude, with anomaly correlation values generally larger than the predictability threshold (0.6) above ~50 hPa. The increase in predictability with altitude is associated with the growing amplitude with height of the large-scale planetary waves that mainly determine the circulation in the region (Andrews et al. 1987). The larger amplitude of these waves in wintertime also explains the larger predictability obtained in the SH. Results indicate that the impact of incorporating ozone interactivity generally contributes to increasing the temperature
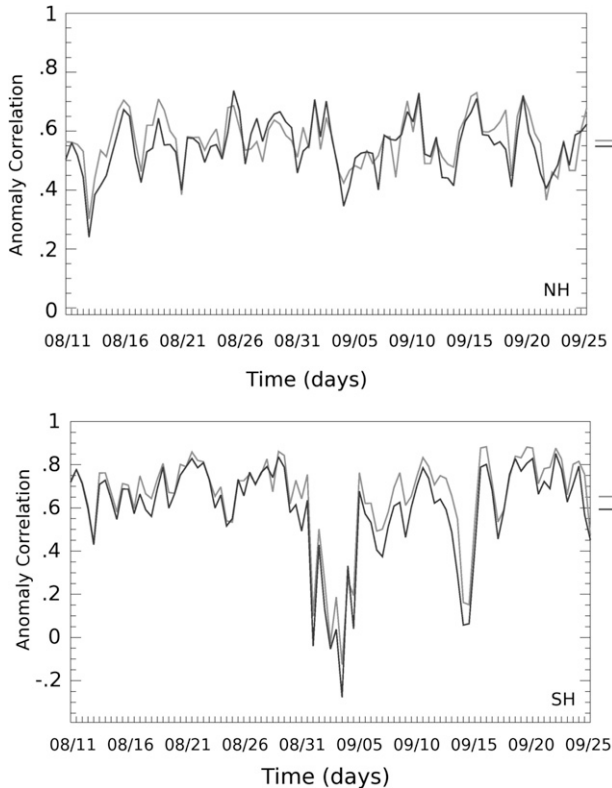
FIG. 9. Time series of temperature anomaly correlation for 10-day forecasts at 50 hPa. Results from noninteractive forecasts using C1 analyses (black) and interactive forecasts using C2 analyses (gray); (top) NH (20°–90°N) and (bottom) SH (20°–90°S) for 11 Aug–25 Sep 2003.
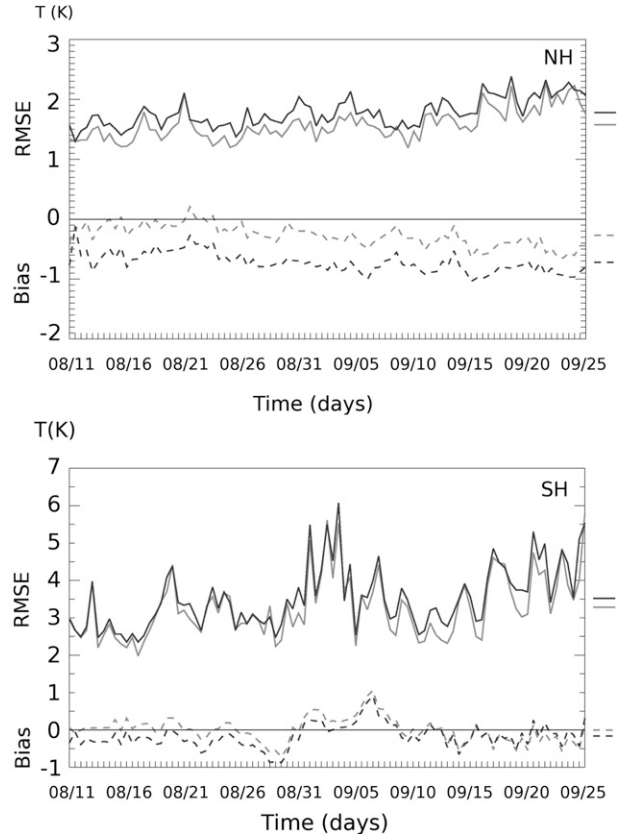

FIG. 10. Time series of temperature RMS error (solid) and biases (dashed) for 10-day forecasts at 50 hPa. Results from noninteractive forecasts using C1 analyses (black) and interactive forecasts using C2 analyses (gray). (top) NH (20°–90°N) and (bottom) SH (20°–90°S) for 11 Aug–25 Sep 2003.

predictability throughout the lower stratosphere. The most significant response is obtained in the NH summertime where there is a systematic improvement at all levels and all time scales from day 3 onward. The largest impact is obtained at 50 hPa where ozone heating increases the predictability by more than 1 day. The impact of ozone heating on temperatures is seen at levels as low as 100 hPa in the NH summertime, where systematic improvements on temperature predictability are obtained for the various time scales. In the SH, the impact of using ozone analyses is nearly neutral except at 50 hPa, where significant improvements are observed.

The benefit of using an NWP model with prognostic ozone on temperature predictability depends on the quality of the ozone distribution, which varies in different regions. To assess it, Fig. 8 compares temperature forecasts produced with the noninteractive assimilation system (A1) with the ones obtained with the ozone interactive system (A2). It shows that the use of prognostic ozone improves the temperature anomaly correlation in the NH but deteriorates it in the SH throughout the lower stratosphere. This negative impact is

mostly eliminated with the incorporation of ozone assimilation (Fig. 7), which suggests that it is associated with biases in the ozone distribution.

Figure 9 presents the time series of anomaly correlations in the extratropics at 50 hPa for the 10-day forecasts launched from the C1 and C2 analyses. Results are presented from 11 August to 25 September 2003 to show the long-term behavior of both assimilation systems. These results indicate a high level of predictability (large anomaly correlation values), with significant temporal variability associated with the strong variation in the dynamical regime throughout the period. The largest predictability is obtained in the SH where we observe the presence of large-scale systems that are well resolved by the model. The anomaly correlation minima that occur in early and mid-September in the SH are indeed characterized by a slight spatial displacement of the polar vortex. Results show that ozone interactivity systematically improves the temperature predictability in both hemispheres throughout the period. In the SH wintertime, the impact is particularly

significant in September when ozone heating becomes significant, whereas in the NH summertime the improvement is more systematic throughout the period. Figure 10 presents the associated time series of the RMS errors and biases during the period for both experiments, which similarly show a significant reduction of the RMS error and half a degree reduction of the temperature bias.

5. Conclusions

The goal of the study is to evaluate the impact of incorporating the radiative feedback from ozone analyses on temperature predictability throughout the stratosphere. Experiments are done with a comprehensive coupled assimilation system that takes into account the full complexity of the dynamical–radiative and photochemical interactions. The incorporation of the radiative feedback from ozone analyses within the coupled model improves several aspects of temperature forecasting in different regions. The improvement of short-term temperature predictability is particularly significant in the SH lower stratosphere where the ozone photochemical lifetime is much larger than the radiative time scale. At longer time scales, the most significant response is obtained in the NH summertime throughout most of the lower stratosphere. The maximum impact in the region is obtained at 50 hPa where there is an increase of the temperature predictability by more than 1 day, which comes from a better representation of ozone radiative heating. Results show a systematic improvement of temperature RMS errors and biases, particularly in the lower stratosphere where changes are significant. This comprehensive coupled 3D-Var assimilation system can be used as a benchmark for the development of linearized methods to address the assimilation of ozone measurements in NWP systems.

REFERENCES

Andrews, D. G., J. R. Holton, and C. B. Leovy, 1987: *Middle Atmosphere Dynamics.* Academic Press, 489 pp.

Austin, J., and Coauthors, 2003: Uncertainties and assessments of chemistry–climate models of the stratosphere. *Atmos. Chem. Phys.,* **3,** 1–27.

Baier, F., T. Erbertseder, O. Morgenstern, M. Bittner, and G. Brasseur, 2005: Assimilation of MIPAS observations using a three-dimensional global chemistry transport model. *Quart. J. Roy. Meteor. Soc.,* **613,** 3529–3542.

Brasseur, G., and S. Solomon, 1986: *Aeronomy of the Middle Atmosphere.* 2nd ed. D. Reidel, 452 pp.

Cariolle, D., and M. Déqué, 1986: Southern Hemisphere medium-scale waves and total ozone disturbances in a spectral general circulation model. *J. Geophys. Res.,* **91** (D10), 10 825–10 846.

——, and J.-J. Morcrette, 2006: A linearized approach to the radiative budget of the stratosphere: Influence of the ozone distribution. *Geophys. Res. Lett.,* **33,** L05806, doi:10.1029/2005GL025597.

Côté, J., S. Gravel, A. Méthot, A. Patoine, M. Roch, and A. Staniforth, 1998: The operational CMC–MRB Global Environmental Multiscale (GEM) model. Part I: Design considerations and formulation. *Mon. Wea. Rev.,* **126,** 1373–1395.

Daerden, F., N. Larsen, S. Chabrillat, Q. Errera, S. Bonjean, D. Fonteyn, K. Hoppel, and M. Fromm, 2007: A 3D CTM with detailed online PSC microphysics: Analysis of the Antarctic winter 2003 by comparison with satellite observations. *Atmos. Chem. Phys.,* **7,** 1755–1772.

Damian, V., A. Sandu, A. Damian, F. Potra, and G. Carmichael, 2002: The kinetic preprocessor KPP—A software environment for solving chemical kinetics. *Comput. Chem. Eng.,* **26,** 1567–1579.

De Grandpré, J., S. R. Beagley, V. I. Fomichev, E. Griffioen, J. C. McConnell, A. S. Medvedev, and T. G. Shepherd, 2000: Ozone climatology using interactive chemistry: Results from the Canadian Middle Atmosphere Model. *J. Geophys. Res.,* **105** (D21), 26 475–26 491.

Dethof, A., 2003: Assimilation of ozone retrievals from the MIPAS instrument on board ENVISAT. ECMWF Tech. Memo. 428, 17 pp.

Errera, Q., F. Daerden, S. Chabrillat, J. C. Lambert, W. A. Lahoz, S. Viscardy, S. Bonjean, and D. Fonteyn, 2008: 4D-Var assimilation of MIPAS chemical observations: Ozone and nitrogen dioxide analyses. *Atmos. Chem. Phys. Discuss.,* **8,** 8009–8057.

Eyring, V., and Coauthors, 2005: A strategy for process-oriented validation of coupled chemistry–climate models. *Bull. Amer. Meteor. Soc.,* **86,** 1117–1133.

Fischer, H., and H. Oelhaf, 1996: Remote sensing of vertical profiles of atmospheric trace constituents with MIPAS limb emission spectrometers. *Appl. Opt.,* **35,** 2787–2796.

Fortuin, J. P. F., and H. Kelder, 1998: An ozone climatology based on ozonesonde and satellite measurements. *J. Geophys. Res.,* **103,** 31 709–31 734.

Gauthier, P., M. Buehner, and L. Fillion, 1999a: Background-error statistics modeling in 3D variational data assimilation scheme: Estimation and impact on analyses. *Proc. ECMWF Workshop on Diagnosis of Data Assimilation Systems,* Reading, United Kingdom, ECMWF, 131–145.

——, C. Charette, L. Fillion, P. Koclas, and S. Laroche, 1999b: Implementation of a 3D variational data assimilation system at the Canadian Meteorological Centre. Part I: The global analysis. *Atmos.–Ocean,* **37,** 103–156.

Geer, A. J., and Coauthors, 2006: The ASSET intercomparison ozone analyses: Method and first results. *Atmos. Chem. Phys.,* **6,** 5445–5474.

Hairer, E., and G. Wanner, 1996: *Solving Ordinary Differential Equations II: Stiff and Differential-Algebraic Problems*. 2nd ed. Springer Series in Computational Mathematics, Vol. 14, Springer, 614 pp.

Hines, C. O., 1997a: Doppler-spread parameterization of gravity-wave momentum deposition in the middle atmosphere. Part 1: Basic formulation. *J. Atmos. Sol. Terr. Phys.,* **59,** 371–386.

——, 1997b: Doppler-spread parameterization of gravity-wave momentum deposition in the middle atmosphere. Part 2: Broad and quasi monochromatic spectra and implementation. *J. Atmos. Sol. Terr. Phys.,* **59,** 387–400.

Hollingsworth, A., and P. Lönnberg, 1986: The statistical structure of short-term forecast errors as determined from radiosonde data. Part I: The wind field. *Tellus,* **38A,** 111–136.

Jackson, D., 2004: Improvements in ozone data assimilation at the Met Office. Met Office Forecasting Research Tech. Rep. 454, 23 pp.

Jonsson, A. I., J. de Grandpré, V. I. Fomichev, J. C. McConnell, and S. R. Beagley, 2004: Doubled CO_2-induced cooling in the middle atmosphere: Photochemical analysis of the ozone radiative feedback. *J. Geophys. Res.,* **109,** D24103, doi:10.1029/2004JD005093.

Li, J., and H. W. Barker, 2005: A radiation algorithm with correlated-k distribution. Part I: Local thermal equilibrium. *J. Atmos. Sci.,* **62,** 286–309.

Long, C. S., A. J. Miller, H.-T. Lee, J. D. Wild, R. C. Przywarty, and D. Hufford, 1996: Ultraviolet index forecasts issued by the National Weather Service. *Bull. Amer. Meteor. Soc.,* **77,** 729–748.

Mathison, C., D. R. Jackson, and M. Keil, 2007: Methods of improving the representation of ozone in the Met Office Model. Met Office Forecasting Research Tech. Rep. 502, 27 pp.

McLinden, C. A., S. C. Olsen, B. Hannegan, O. Wild, M. J. Prather, and J. Sundet, 2000: Stratospheric ozone in 3-D models: A simple chemistry and the cross-tropopause flux. *J. Geophys. Res.,* **105** (D11), 14 653–14 665.

Ménard, R., and Coauthors, 2007: Coupled chemical–dynamical data assimilation: Final Report. ESA/ESTEC Contract 185604/NL/FF, 458 pp.

Morcrette, J.-J., 2003: Ozone–radiation interactions in the ECMWF forecast system. ECMWF Tech. Memo. 375, 36 pp.

Murphy, A. H., and E. S. Epstein, 1989: Skill scores and correlation coefficients in model verification. *Mon. Wea. Rev.,* **117,** 572–581.

Parrish, D. F., and J. C. Derber, 1992: The National Meteorological Center's spectral statistical interpolation analysis system. *Mon. Wea. Rev.,* **120,** 1747–1763.

Raspollini, P., and Coauthors, 2006: MIPAS level-2 operational analysis. *Atmos. Chem. Phys.,* **6,** 5605–5630.

Ridolfi, M., and Coauthors, 2007: Geophysical validation of temperature retrieved by the ESA processor from MIPAS/ENVISAT atmospheric limb-emission measurements. *Atmos. Chem. Phys.,* **7,** 4459–4487.

Riishøjgaard, L. P., 1996: On four-dimensional variational assimilation of ozone data in weather prediction models. *Quart. J. Roy. Meteor. Soc.,* **122,** 1545–1571.

Sander, S. P., and Coauthors, 2003: Chemical kinetics and photochemical data for use in atmospheric studies. JPL Publication 02-25, Evaluation 14, Jet Propulsion Laboratory, 334 pp.

Sassi, F., B. A. Boville, D. Kinnison, and R. R. Garcia, 2005: The effects of interactive ozone chemistry on simulations of the middle atmosphere. *Geophys. Res. Lett.,* **32,** L07811, doi:10.1029/2004GL022131.

Ward, W. E., J. Oberheide, M. Reise, P. Preusse, and D. Offerman, 2000: Planetary wave two signatures in CHRISTA 2 ozone and temperature data. *Atmospheric Science across the Stratopause,* D. E. Siskind, S. D. Eckermann, and M. E. Summers, Eds., Amer. Geophys. Union, 319–325.

WMO, 1998: Commission for Basic Systems extraordinary session (1998) abridged final report with resolutions and recommendations. WMO Rep. 893, 179 pp.

——, 2007: Scientific assessment of ozone depletion 2006. WMO Rep. 50, Global Ozone Research and Monitoring Project, 572 pp.